Available online at www.sciencedirect.com
SCIENCE DIRECT®
Sensors and Actuators B xxx (2005) xxx–xxx
SENSORS AND ACTUATORS B CHEMICAL
www.elsevier.com/locate/snb

A label-free biosensor-based cell attachment assay for characterization of cell surface molecules

Bo Lin [a], Peter Li [a], Brian T. Cunningham [b,*]

[a] *SRU Biosystems, 14A Gill Street, Woburn, MA 61801, USA*
[b] *Department of Electrical and Computer Engineering, University of Illinois at Urbana-Champaign, Micro and Nanotechnology Laboratory, 208 N. Wright Street, Urbana, IL 61801, USA*

Received 22 December 2004; received in revised form 1 April 2005; accepted 13 April 2005

Abstract

A photonic crystal optical biosensor is incorporated into standard format 96-well microplates for the purpose of detecting the attachment of cells to the biosensor surface without the use of fluorescent labels or any other type of marker. We show that the attachment of cells to the biosensor can be modulated by the immobilization of cognizant ligands to the sensor surface that selectively recognize expressed outer membrane proteins. Jurkat T cells were used as a model system for demonstrating the biosensor-based assay. The attachment of two Jurkat cell lines were compared versus surface-immobilized monoclonal antibodies, where the expression level of cell surface antigens correlated well with the level of cell attachment to sensors with the corresponding antibody. The biosensor system was able to distinguish nearly identical Jurkat cell lines, which only differed by the presence of one expressed surface marker. These results suggest that the biosensor detection system can be used to identify cell surface molecules and to screen ligands that interact with cell surface molecules.

Keywords: Biosensor; Label-free; Cell attachment assay; Cell–protein interactions

1. Introduction

Identification of protein–cell interactions will help to elucidate the mechanisms that are involved in cellular functions, such as inflammation, wound healing, cancer metastasis, cell differentiation and migration [1–3]. Current techniques for studying cell–protein interactions are quite time consuming and labor intensive [4–8]. These processes usually involve many steps, including radioisotope or fluorescence labeling, blocking, washing, and detection. While optical biosensors based upon surface plasmon resonance have been used for many years to characterize macromolecular affinity interactions [9], they have not found widespread usage for detecting cells for several reasons. The detection system is arranged only to interrogate a small (<1 mm^2) region of the sensor surface within a narrow (~50 μm wide × 50 μm tall) flow channel under a constant flow of buffer. Blockage of the flow channel by cells, low assay throughput, and assay conditions not amenable to maintaining viable cells (such as lack of incubation) have prevented biosensor-based methods from becoming widely adopted.

A new class of optical biosensors based on the unique properties of optical device structures known as "photonic crystals" have been recently developed [10,11]. A photonic crystal is composed of a periodic arrangement of dielectric material in two or three dimensions [12,13]. If the periodicity and symmetry of the crystal and the dielectric constants of the materials used are chosen appropriately, the photonic crystal will selectively couple at particular wavelengths, while transmitting others [14]. A photonic crystal structure geometry can be designed to concentrate light into extremely small volumes and to obtain very high local electromagnetic field intensities. These devices are often referred to as "sub-wavelength surfaces (SWS)" or as "nanostructure surfaces" because typical dimensions are smaller than the wavelength of light that

* Corresponding author. Tel.: +1 217 265 6291; fax: +1 217 244 6375.
E-mail address: bcunning@uiuc.edu (B.T. Cunningham).

0925-4005/$ – see front matter © 2005 Elsevier B.V. All rights reserved.
doi:10.1016/j.snb.2005.04.022

they manipulate. As shown in previous publications, the photonic crystal biosensor behaves as a narrowband wavelength reflectance filter, where the sensor reflects ~100% of incident light at the resonant wavelength, while all other wavelengths are transmitted through the sensor structure.

The sensor operates by measuring changes in the wavelength of reflected light as biochemical or cellular binding events take place on the surface. For example, when a protein is immobilized on the sensor surface, an increase in the reflected wavelength is measured when a complementary binding protein is exposed to the sensor. Using low-cost components, the readout instrument is able to resolve protein mass changes on the surface with resolution less than 1 pg/mm^2. While this level of resolution is sufficient for measuring small-molecule interactions with immobilized proteins, the dynamic range of the sensor is large enough to also measure larger biochemical entities including live cells, cell membranes, viruses, and bacteria. A sensor measurement requires ~20 ms, so large numbers of interactions can be measured in parallel, and kinetic information can be gathered. The reflected wavelength of the sensor can be measured either in "single point mode" (such as for measuring a single interaction within a microplate), or an imaging system can be used to generate an image of a sensor surface with ~13 μm pixel resolution. The "imaging mode" can be used for applications that increase the overall resolution and throughput of the system such as label-free microarrays, self-referencing microplates, and multiplexed spots/well [15]. The sensors are inexpensively manufactured on continuous sheets of plastic film, and incorporated into standard microplates that are compatible with cell culture methods and standard microplate handling procedures.

2. Materials and methods

2.1. Biosensor and detection system

The biosensor-embedded microplates were manufactured using the sensor design and fabrication methods reported previously [16]. Two styles of biosensor readout instrumentation were used to perform the assays, both of which measure changes in the peak wavelength value (PWV) of the biosensor surface as the detected output. The primary instrument (referred to here as the "Plate Reader") measures in single point mode, where the biosensor is illuminated with a ~2 mm diameter beam of white light from a fiber optic probe, and reflected light is gathered by a second fiber optic adjacent to the illuminating fiber. The Plate Reader reports an averaged PWV shift for the center 2 mm region of each microplate well, representing the density of attached cells within the detection zone. By combining eight illumination/detection fiber probes in parallel, a single column of the microplate is measured simultaneously, and an entire plate can be scanned at 30 s intervals. The secondary instrument (referred to here as the "Imager") replaces the single point optical fiber illumination/detection with an optical system capable of measuring PWV shifts on a pixel-by-pixel basis that can generate images of PWV shift with a spatial resolution as low as 9 μm × 9 μm. Rather than providing a measurement representing averaged cell attachment over a large area, the Imager measures the density of cell binding as a function of position within the microplate well. The design of both the Plate Reader and the Imager have been reported previously [10,15].

2.2. Cell cultures and antibodies

Human acute T cell leukemia cells E6-1 and J45.1, a CD45 deficient variant of the E6-1 clone, were ordered from ATCC. Both cell clones were maintained in RPMI1640 medium (ATCC) with 10% FBS. Hybridoma CRL-1606 (ATCC) was cultured in DMEM (Dulbecco's modified Eagle's medium) with 10% newborn bovine calf serum. Monoclonal antibodies in this study were purchased from R&D systems Inc., which include anti-human CD3 (MAB100), anti-human CD28 (MAB342), anti-human CD45 (MAB1430), anti-human CTLA4 (cytotoxic T lymphocyte-associated molecule-4, MAB325), control isotype antibodies, and anti-mouse CD3 antibodies (MAB484). Antibody stock solutions were prepared in phosphate-buffered saline (PBS), pH 7.4 at a concentration of 1 mg/ml and diluted to preferred concentration before coating.

2.3. Biosensor-based cell attachment assay

A two-step biosensor cell attachment protocol was developed as illustrated in Fig. 1. First, the sensor surface at the bottom of the microplate wells were coated with an immobilized antibody. Second, cells were introduced into the microplate wells, where they have the opportunity to bind with the immobilized antibody.

The antibody immobilization step was performed by incubating a 100 μl volume of the antibody reagent in the well at a concentration of 10 μg/ml for 60 min. The biosensor PWV response is monitored during the antibody immobilization step using the Plate Reader to verify stable and uniform of coating. Where indicated, negative control antibodies were

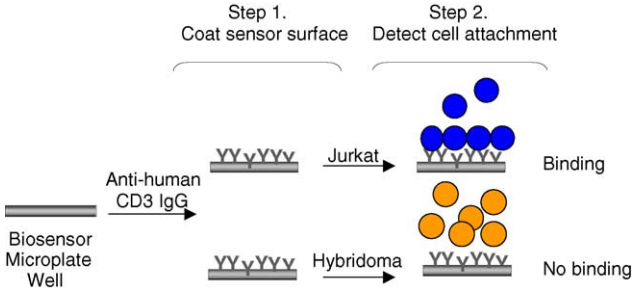

Fig. 1. Schematic design of the label-free biosensor cell attachment assay.

immobilized in selected wells to verify that a signal is not produced by attachment of cells to unrecognized antibodies.

After removing the solution from the wells and rinsing the sensor surface with immobilization buffer, the coated sensor surface was prepared for the second step of the assay process by incubation with cell culture media RPMI1640 supplemented with 10% fetal bovine serum (ATCC 30-2020) and penicillin-streptomycin glutamine (Sigma, P0781). Suspension cells were harvested and diluted in RPM1640 complete media with 10% fetal bovine serum (FBS). Different numbers of cells were then applied into antibody-coated sensor wells. Cell attachment was monitored in real-time using the Plate Reader instrument as the suspension cells bound to the coated surface via affinity interaction of cell surface antigen and the antibody immobilized on the sensor surface.

2.4. Miniaturization of the cell attachment assay

For the miniaturized biosensor cell assay, the first step of the assay process was altered. Rather than immobilize the antibody on the entire bottom surface of the microplate well, only a 1 μl droplet of the antibody solution was applied to the biosensor using a pipette tip. Because the droplet only coats antibody onto a portion of the well, a second negative control antibody droplet was applied next to the binding antibody, and the Imager instrument was used to measure the difference in binding between the positive and negative control locations within the well.

Two kinds of T lymphocyte cells, Jurkat E6-1 (ATCC, TIB-152) and J45.01 (ATCC, CRL-1990), were maintained in RPMI1640 culture media as previously described. Cells were harvested and resuspended at 5×10^6 cells/ml in fresh RPMI complete media. The 10^5 cells were added into antibody droplet-coated wells. The Imager instrument was used to record changes in reflected PWV from the biosensor as a function of time at 1 min intervals while the cells attach to the sensor surface. After an incubation of 60 min, a final wash with buffer was used to remove any weakly bound cells, and the final PWV shift was measured. For each antibody/cell combination, eight replicate wells were used, and errors are reported as standard deviation over the eight replicate data points.

Table 1 summarizes the matrix of antibody/cell interactions that were investigated in this experiment, with expected outcome ("+" for binding, "−" for no binding).

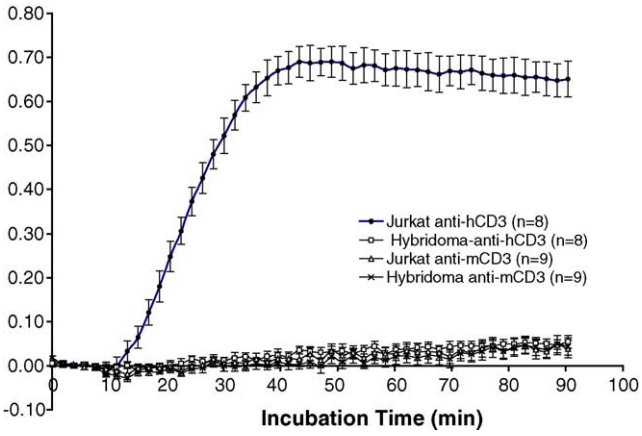

Fig. 2. The 2×10^5 Jurkat cells were added to wells coated with anti-human CD3, anti-mouse CD3, and mouse IgG. Specific attachment of Jurkat cells to anti-human CD3 monoclonal antibody-coated sensor surface was detected while binding of Jurkat cells to anti-mouse CD3 or mouse control IgG was not measurable.

3. Results

3.1. Specific interaction of immobilized antibodies and Jurkat cell surface antigens

As a simple illustration of the detected signal from the biosensor, the interaction matrix of three immobilized antibodies (Mouse IgG, Anti-Mouse CD3, and Anti-Human CD3) with Jurkat cells was measured using the Plate Reader instrument and biosensor-embedded 96-well microplates. After the cells were added to the wells, the shift of biosensor PWV was monitored as a function of time for 90 min at ∼1 min intervals. As shown in Fig. 2, the PWV increases steadily until reaching a plateau of $\Delta\text{PWV} \sim 1.65$ nm after 45 min of incubation for the Jurkat:ahCD3 interaction while the Jurkat:mIgG, and Jurkat:amCD3 produce no measurable shift in PWV. The binding of cells to the antibody-coated sensor was clearly detected only when the corresponding antigen was expressed on the Jurkat cell surface. While continuous measurement over the 90 min incubation period was performed in this fashion for all the antibody–cell interactions studied, for simplicity we shall report only the "end point" measurement, where the endpoint signal is calculated as $\Delta\text{PWV} = \text{PWV}(t = 90\,\text{min}) - \text{PWV}(t = 0)$.

The interactions of antibodies with cell surface antigens were monitored in real-time as lymphocytes bound to the coated sensor surface. The binding of cells to the antibody-

Table 1
Matrix of immobilized antibody/cell combinations investigated

Cell/antibody	Mouse IgG (control)	Anti-mouse CD3	Anti-human CD3	Anti-human CD28	Anti-human CD45	Anti-human CTLA4
Hybridoma	–	–	–	X	X	X
Jurkat E6-1	–	–	+	+	+	–
Jurkat J45.01	–	–	+	+	–	–

The "+" indicates that expressed outer surface proteins on the cell are expected to bind to the immobilized ligand, while "−" entries indicate that binding is not expected between the cell and the ligand. An "X" entry indicates a cell/protein combination that was not studied.

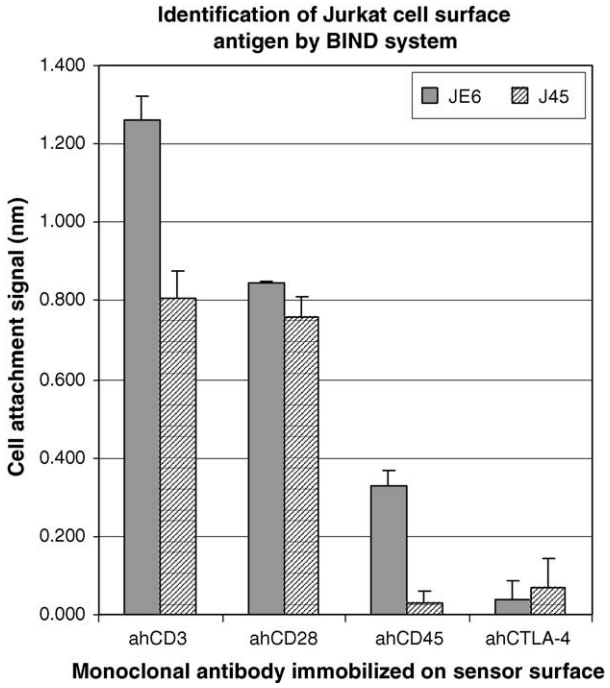

Fig. 3. Identification of cell surface antigens using the label-free cell attachment assay. Jurkat cells (5×10^5) were added in the wells that have been coated with anti-human CD3, anti-human CD28, anti-human CD45, and anti-human CTLA-4 monoclonal antibodies. Cell attachment was detected using BIND microplate reader in real-time. After 60 min. incubation, unattached cells were removed and plate was washed with RPMI1640 complete growth media. Endpoint cell attachment was analyzed using BIND EMS software. Solid bars represent Jurkat E6.1 cell and striped bars represent cell attachment data collected from J45.01.

coated sensor was clearly detected by the Plate Reader only when corresponding antigen was expressed on the Jurkat cell surface as shown in Fig. 3. This data shows that biosensor surfaces coated with the anti-human CD45 antibody specifically recognize the difference between the Jurkat clones, where Jurkat E6-1 expresses CD45 and Jurkat J45.1 is CD45 deficient.

3.2. Inhibition of Jurkat cell binding

The label-free cell-attachment assay method was also used to demonstrate that the binding of cells to the sensor surface could be modulated by the presence of competing antibodies in the test sample. As shown in Fig. 4, Jurkat cell binding to an anti-human CD3 coated sensor surface was inhibited by adding anti-human CD3 IgG to the reaction buffer. As shown in Fig. 4, anti-human CD3-induced Jurkat cell attachment was reduced in the presence of increasing concentrations of anti-human CD3 antibody.

3.3. Miniaturization of the cell attachment assay using the Imager instrument

The format for the cell attachment assay can be further optimized so that only 1 μl of IgG is needed to pattern protein

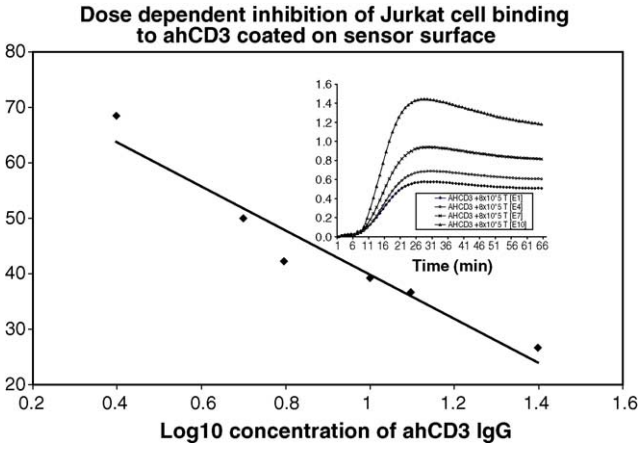

Fig. 4. Inhibition of Jurkat cell binding to immobilized CD3 by the addition of anti-human CD3 antibody to the test sample. The inhibition percentage characterizes the percentage of cell binding density that occurs in the presence of the antibody compared to the cell binding density that occurs without the antibody. The inset shows kinetic sensor data for various concentrations.

within each microplate well. The modified assay procedure requires immobilization of the ligand onto only a portion of the biosensor surface at the bottom of the well in the form of a small droplet. The droplet results in an "active" region of the sensor surface that is capable of selectively capturing Jurkat cells from the test sample. Using the Imager readout instrument, selective binding of Jurkat cells to the active portions of the biosensor microplate well can be detected. Through the use of multiple active regions within the well, each containing a different immobilized ligand, the interaction of a cell population with multiple proteins may be analyzed simultaneously.

To illustrate this concept, two active regions were created by the deposition of two separate 1 μl droplets of anti-human CD3 and anti-mouse CD3 at a concentration of 1 mg/ml. The droplets were allowed to incubate on the biosensor surface for 60 min before the well was washed thoroughly with PBS buffer. The Imager instrument was used to scan the PWV as a function of position inside the well with a pixel resolution of 13 μm × 13 μm, both before and after the ligand immobilization. The PWV images were subtracted to yield an image representing the spatial map of ligand binding in the bottom of the well, shown in Fig. 5a. In Fig. 5a, the PWV shift due to ligand binding is represented by a grey scale image, where lighter regions indicate areas of highest PWV shift. The anti-human CD3 spot produces a positive PWV shift of 1.15 nm, and the anti-mouse CD3 spot produces a positive PWV shift of 1.98 nm. Following the second PWV scan of the well, the well was filled with Jurkat 1×10^5 cells and allowed to incubate for 20 min. After 20 min, a third PWV scan of the well was performed. The second (post immobilization ligand) PWV image was mathematically subtracted on a pixel-by-pixel basis from the third image to yield Fig. 5b, which represents the PWV shift 0f 0.48 nm caused by Jurkat cell binding to the immobilized antibodies. Lighter regions

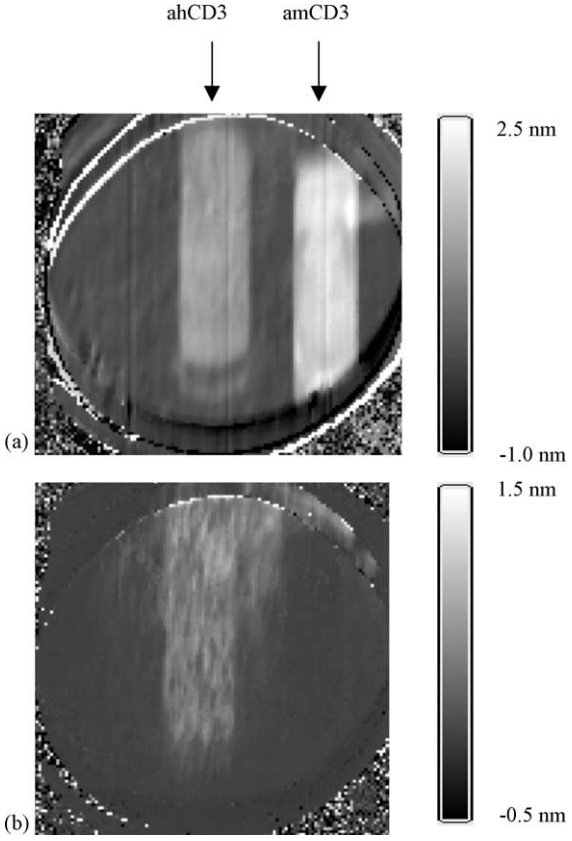

Fig. 5. Specific Jurkat cell capture by CD3. (a) Two regions within a well are coated with ahCD3 and amCD3, resulting in average PWV shift of 1.15 and 1.98 nm, respectively. (b) Jurkat cell attachment to ahCD3, with an average PWV shift of 0.48 nm, while no cell attachment is present on amCD3.

on the grey scale image represent pixels with the greatest PWV shift due to cell binding. Fig. 5b clearly demonstrates that Jurkat cells only interact with the defined area that has been coated with anti-human CD3 while no detectable PWV shift was measured from the spot with anti-mouse CD3 monoclonal antibody.

4. Discussion

In this work, we have demonstrated that an optical biosensor label-free assay system embedded into a standard 96-well microplate provides a simple, convenient format for studying protein–cell interactions. Immobilized antibodies on the sensor surface retain their ability to selectively bind with cell surface antigens expressed by Jurkat T-cells, and through the binding interaction to selectively attach the cell to the sensor surface where it can be detected. We have shown that nonspecific binding of T-cells to unrecognized proteins on the sensor surface is not measurable. The biosensor system was able to distinguish Jurkat E6-1 cells from nearly identical J45.01 cells, which only differ by the expression of CD45 by the E6-1 cell line. The binding specificity of cell surface antigen and immobilized antibody was further tested using a competition assay where cell attachment was carried out in the presence of corresponding antibody in the binding buffer.

The biosensor-based detection method provides a highly quantitative means for determining the density of bound cells without the use of labels or stains for visualization. The detection of cell density, therefore, does not require the addition of reagents that may adversely affect the cell population, allowing the same cells to be measured multiple times, or to allow recovery of the cells.

Used in this way, the biosensor microplate may be used to perform a function similar to a flow cytometer system from the standpoint that cells can be specifically recognized by their interaction with an antibody tag. Compared to a flow cytometer, the biosensor microplate system would be advantageous because the cell recognition function is performed without the use of fluorescent tags, and the throughput of the system is such that a new microplate can be scanned by the system every ∼60 s. Because the biosensors are embedded in the microplate format from a manufacturing process based upon plastic materials that are fabricated on a square-yardage basis, the biosensor microplates are intended to be disposed of after a single usage. The microplate format is compatible with standard liquid handling equipment, incubation chambers, and plate washers—unlike flow-cell-based biosensor approaches that require serial addition of samples into a microfluidic channel.

In this report, we have demonstrated the use of a rudimentary two-element “array” of two different ligands immobilized within the same microplate well. In addition to reducing the quantity of monoclonal antibody required for performing the cell attachment assay, the use of immobilized spots within a well enables multiplexed comparison of the attachment of a cell population to a group of antibodies. The multiplexed assay is enabled by the Imager instrument which is capable of measuring cell binding density distribution within the well. Although an assay using only a single well with two separate immobilized antibody spots deposited manually by pipette was shown here, this type of approach could be extended to >50 spots/well using appropriate commercial spot deposition equipment.

References

[1] L.M. Coussens, Z. Werb, Inflammation and cancer, Nature 420 (2002) 860–867.
[2] A. Moustakas, K. Pardali, A. Gaal, C.-H. Heldin, Mechanisms of TGF-[beta] signaling in regulation of cell growth and differentiation, Immunol. Lett. 82 (2002) 85–91.
[3] D.A. Lauffenburger, A.F. Horwitz, Cell migration: a physically integrated molecular process, Cell 84 (1996) 359–369.
[4] K.W.S.E.U. Eppenberger, Quantification of cells cultured on 96-well plates, Anal. Biochem. 182 (1989) 16–19.
[5] M. Malmqvist, BIACORE: an affinity biosensor system for characterization of biomolecular interactions, Biochem. Soc. Trans. 27 (1999) 335–340.
[6] L.S. De Clerck, C.H. Bridts, A.M. Mertens, M.M. Moens, W.J. Stevens, Use of fluorescent dyes in the determination of adherence of

human leucocytes to endothelial cells and the effect of fluorochromes on cellular function, J. Immunol. Meth. 172 (1994) 115–124.
[7] D.B. Bylund, L.C. Murrin, Radioligand saturation binding experiments over large concentration ranges, Life Sci. 67 (2000) 2897–2911.
[8] D.B. Bylund, M.L. Toews, Radioligand binding methods: practical guide and tips, Am. J. Physiol. Lung Cell Mol. Physiol. 265 (1993) L421–L429.
[9] M.A. Cooper, Label-free screening of bio-molecular interactions, Nature 377 (2003) 834–842.
[10] B.T. Cunningham, P. Li, B. Lin, J. Pepper, Colorimetric resonant reflection as a direct biochemical assay technique, Sens. Actuators B 81 (2002) 316–328.
[11] A.J. Haes, R.P.V. Duyne, A nanoscale optical biosensor: sensitivity and selectivity of an approach based on the localized surface plasmon resonance spectroscopy of triangular silver nanoparticles, J. Am. Chem. Soc. 124 (2002) 10596–10604.
[12] J.D. Joannopoulos, R.D. Meade, J.N. Winn, Photonic Crystals, Princeton University Press, Princeton, NJ, 1995.
[13] B.A. Munk, Frequency Selective Surfaces, Wiley, 2000.
[14] V. Pacradouni, W.J. Mandeville, A.R. Cowan, P. Paddon, J.F. Young, S.R. Johnson, Photonic band structure of dielectric membranes periodically textured in two dimensions, Phys. Rev. B 62 (2000) 4204–4207.
[15] P. Li, B. Lin, J. Gerstenmaier, B.T. Cunningham, A new method for label-free imaging of biomolecular interactions, Sens. Actuators B 99 (2004) 6–13.
[16] B.T. Cunningham, P. Li, S. Schulz, B. Lin, C. Baird, J. Gerstenmaier, C. Genick, F. Wang, E. Fine, L. Laing, Label-free assays on the BIND system, J. Biomol. Screen. 9 (2004) 481–490.